Strong contributions of indirect processes to the electron-impact ionization cross section of Sc$^+$ ions

J. Jacobi, H. Knopp, S. Schippers, and A. Müller

Institut für Atom- und Molekülphysik, Justus-Liebig-Universität Giessen, D-35392 Giessen, Germany

S. D. Loch, M. Witthoeft, and M. S. Pindzola

Department of Physics, Auburn University, Auburn, Alabama 36849, USA

C. P. Ballance

Department of Physics, Rollins College, Winter Park, Florida 32789, USA

We present experimental measurements and theoretical calculations for the electron-impact single ionization cross section of Sc$^+$ ions covering an energy range from threshold to 1000 eV. An electron-ion crossed-beams setup was employed for the measurements of absolute cross sections as well as for a high-resolution energy scan to uncover fine details in the energy dependence of the cross section. Direct ionization is described by configuration-averaged distorted-wave theory and indirect ionization by R-matrix theory. Indirect processes contribute to the total ionization cross section by up to $\sim 40\%$. This finding is related to the existence of strong $3p \rightarrow 3d$ excitation channels in Sc$^+$($3p^6 3d 4s$). The shape of the related cross-section feature is reminiscent of the very strong $4d \rightarrow 4f$ excitation, found in the ionization of xenon and its neighboring elements.

I. INTRODUCTION

Electron-impact ionization of ions is a fundamental atomic-collision process. For applications in astrophysics and applied plasma research, ionization cross sections and rate coefficients are needed. For the understanding of ionization processes, a detailed investigation of contributing mechanisms is indispensable. Electron-impact ionization can either proceed via direct removal of outer electrons or indirectly by the excitation or ionization of inner shell electrons with subsequent autoionization. In plasma modeling, indirect ionization processes are often neglected, although they may even dominate the total ionization cross section, as is the case, e.g., for sodiumlike Fe^{15+} ions [1]. For the isoelectronic sequence of lithiumlike ions, it has been found that the importance of indirect ionization processes increases with increasing ion charge [2].

The complexity and enormous variety of possible ionization pathways has resulted in sophisticated theoretical methods for predictions of electron-impact ionization cross sections. For reasons of simplicity, theoretical attempts to describe the most important ionization channels have mainly concentrated on quasi-one-electron systems from the lithium and sodium isoelectronic sequences. Theoretical methods that are to be applied to more complex systems require accurate experimental measurements to establish their reliability. Experimental techniques have been developed that allow for high-precision *absolute* measurements of cross sections with an energy resolution that is sufficient to resolve individual contributions due to indirect ionization mechanisms [3–5].

In general, single ionization of an ion or atom by electron impact results from direct removal of a target electron or from indirect processes characterized by the formation of highly excited intermediate states that decay by electron emission. Here we present a case where indirect processes significantly contribute to the total electron-impact ionization cross section for a singly charged ion, namely Sc$^+$.

Singly and doubly charged scandium ions with the electron configurations [Ar]$3d\,4s$ and [Ar]$3d$, respectively, have a peculiar electronic structure with only one $3d$ electron outside a closed rare-gas core and with strong $3p \rightarrow 3d$ excitation channels leading to the formation of $3p^5 3d^2 4s$ or $3p^5 3d^2$ configurations of Sc$^+$ and Sc^{2+}, respectively. These multiply excited states autoionize efficiently via very fast $3p^5 3d^2 \rightarrow 3p^6$ super-Coster-Kronig transitions. Correspondingly, $3p \rightarrow 3d$ excitation with subsequent autoionization forms strong ionization channels, as has been observed recently in the photoionization cross section of Sc^{2+} ions [6].

II. EXPERIMENT

Electron-impact single ionization cross sections of Sc$^+$ were measured in the energy range 6.5–1000.0 eV. A crossed-beams apparatus was employed for the measurements using the well established animated-beams method for the determination of absolute cross sections [7,8] as well as a high-resolution energy-scan technique to uncover fine details in the energy dependence of cross sections [3]. Measurements covering a maximum electron energy range of 200 eV in a single sweep with up to almost 3000 energy steps were carried out at optimum beam overlap. The number of sweeps was chosen such that statistical uncertainties were reduced to below a desired level. The resulting relative cross sections were then normalized to the absolute cross sections determined by the animated-beams method. The absolute uncertainty of these normalized energy-scan cross sections is therefore almost identical to that of the cross sections ob-
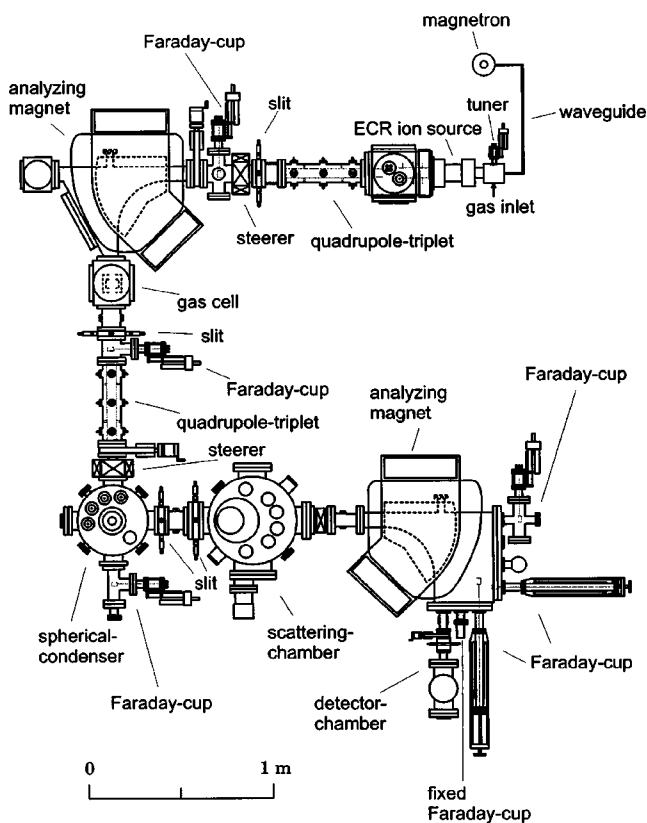
FIG. 1. Schematic drawing of the experimental setup.

tained with the animated-beams method. The experimental setup used for the present measurements was employed recently for detailed measurements on C^{3+} [9] and Mg^+ [10]. A schematic drawing of the experimental setup is shown in Fig. 1.

A 10-GHz all-permanent-magnet ECR ion source [11] is used to produce the required ions from gases or vaporized solids. We used an oven based on an aluminum oxide tube with a heating wire to vaporize the solid scandium. The complete ion source is working on a potential of 12 kV with respect to ground, so that singly charged ions were accelerated to an energy of 12 keV. Behind the extraction electrode and einzel lens, the ion beam can be manipulated with deflection plates, a quadrupole triplet, and a magnetic steerer. The first analyzing magnet selects ions with the desired charge to mass ratio. In this experiment, the gas cell located at the exit aperture of the first magnet was not used. After passing a second quadrupole triplet and magnetic steerer, the ion beam is deflected and focused into the scattering chamber by the spherical condenser. Before entering the scattering chamber, the ion beam is collimated by two slits with 0.8 $\times 0.8$ mm^2 apertures separated from one another by 195 mm. The collimated beam of typically 1 nA is crossed under an angle of 90° with the ribbon-shaped electron beam in the scattering chamber. The high-current electron gun can be moved up and down mechanically. This allows translation of the electron beam through the ion beam, which is required for the determination of absolute cross sections with the animated-beams technique. The ionized product ions were separated from the parent ion beam with a 90° analyzing

magnet and subsequently passed through a 180° electrostatic sector field. The product ions were counted by a channel electron multiplier single-particle detector [12] with a detection efficiency of 97% ±3%. The primary ion beam was collected in a Faraday cup that can be moved to an arbitrary position inside the magnet chamber. In order to optimize the beam transport, the ion current can be measured with four moveable Faraday cups at different positions along the beamline.

A particular experimental feature of the single ionization of Sc^+ ions is a high background count rate due to the presence of autoionizing metastable states in the parent ion beam. These states are produced in the hot plasma of the ECR ion source and have lifetimes longer than the time of flight from the ECR source to the interaction chamber. This resulted in low signal-to-background ratios in the experiment, especially at low electron energies where the electron current and thus the real ionization signal rate is quite low due to space-charge limited electron-beam transport. A voltage-labeling technique was therefore used to separate the product ions ionized in the beam-crossing region from those ions ionized by autoionization or other processes elsewhere on their flight path. An additional voltage of −900 V was applied to the interaction region for that purpose. Thus all Sc^{2+} ions produced in that region from parent Sc^+ ions had a kinetic energy that was lower by 900 eV compared to those created elsewhere. This energy difference is sufficient to separate the two components of the Sc^{2+} product ion beam in the second analyzing magnet and to suppress the background level by more than a factor of 6. At an electron energy of 100 eV, a signal-to-background ratio of 0.39 was obtained at a maximum counting rate of 52.5 kHz without the voltage labeling technique. This ratio was enhanced to 2.64 when the voltage labeling was applied. At higher electron energies, this ratio was even more favorable.

The carefully estimated systematic uncertainty of the absolute cross-section determination is the sum of the systematic uncertainty of the experimental setup with a possible error of 6.3% and the energy dependent determination of the electron current through the interaction region with a possible error of about 15% at 20 eV and less than 1% for energies greater than 120 eV. Typical total uncertainties at electron energies of 30 eV, 90 eV, and 500 eV are 14%, 8%, and 7%, respectively. All energies given in this paper are for the electron-ion center-of-mass system. The systematic uncertainty of the electron energy E_e is at most 1 eV or 0.3% of E_e, whichever is greater.

III. THEORY

The total electron-impact ionization cross section from the initial term i may be represented by

$$\sigma_{\text{tot}} = \sum_f \sigma_d(i \rightarrow f) + \sum_n \sigma_{ex}(i \rightarrow n) \frac{\sum_f A_a(n \rightarrow f)}{\Gamma_n}, \quad (1)$$

where $\sigma_d(i \rightarrow f)$ is the direct ionization cross section between terms i and f, $\sigma_{\text{ex}}(i \rightarrow n)$ is the direct and resonant excitation

cross section between terms i and n, $A_a(n \to f)$ is the Auger transition rate from n to f, and Γ_n is the total decay rate from excited term n. For Sc$^+$, the direct ionization proceeds through removal of a $4s$ or a $3d$ electron and the transitions are represented by reaction pathways such as

$$Sc^+(3p^63d4s) + e^- \to Sc^{2+}(3p^63d) + e^- + e^-, \quad (2)$$

$$\to Sc^{2+}(3p^64s) + e^- + e^-. \quad (3)$$
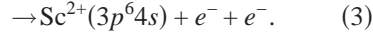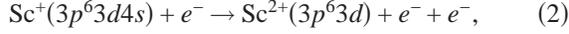
In the present calculations, we use the configuration-average distorted-wave method [13] to evaluate the direct ionization cross sections.

The main direct $3p \to 3d$ excitation followed by autoionization for Sc$^+$ is represented by

$$Sc^+(3p^63d4s) + e^- \to (Sc^+)^*(3p^53d^24s) + e^-$$
$$\to Sc^{2+}(3p^63d) + e^- + e^-, \quad (4)$$
$$\to Sc^{2+}(3p^64s) + e^- + e^-. \quad (5)$$
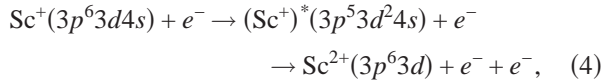
We expect there to be significant excitation autoionization (EA) due to the strong excitation from the $3p$ subshell to the $3d$ subshell. All 38 terms of the $3p^53d^24s$ configuration are autoionizing. The cross section for excitation to autoionizing terms is evaluated in the close-coupling approximation, using the R-matrix method [14,15].

It is also possible to excite the parent ions to autoionizing terms via resonant excitation such as

$$Sc^+(3p^63d4s\ ^3D) + e^- \to Sc(3p^53d^24s\ LS\ nl). \quad (6)$$

This could be followed by a double-autoionization, leaving the ion in charge state Sc^{2+} by a decay process

$$Sc(3p^53d^24s\ LS\ nl) \to Sc^+(3p^53d^24s\ L'S') + e^-, \quad (7)$$
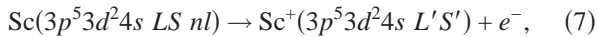
followed by the Auger processes described by Eqs. (4) and (5). Because of the required intermediate autoionizing state, this process can only occur resonantly at energies above the first EA threshold. It is also possible for the resonance terms to autoionize to bound terms of Sc$^+$, and thus not contribute to the ionization cross section. These processes are represented by

$$Sc(3p^53d^24s\ nl) \to Sc^+(3p^63d4s) + e^- \quad (8)$$

$$\to Sc^+(3p^63d^2) + e^- \quad (9)$$

$$\to Sc^+(3p^63dnl) + e^-. \quad (10)$$
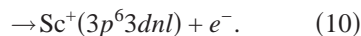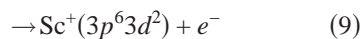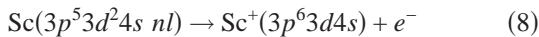
The R-matrix method includes resonant excitation, and some of the possible branching transitions. Thus this last process is naturally included in the excitation cross sections that we calculate. Note that our calculation includes the Auger processes given by Eqs. (8) and (9), but only $nl=4p$ for Eq. (10), due to the configurations which were included.

The theory for the time-independent configuration-average distorted-wave (CADW) method has been described in detail previously; see Pindzola *et al.* [13]. In our implementation of the CADW approach, the configuration-average threshold energies and radial wave functions for the bound configurations are evaluated using the Hartree-Fock relativ-
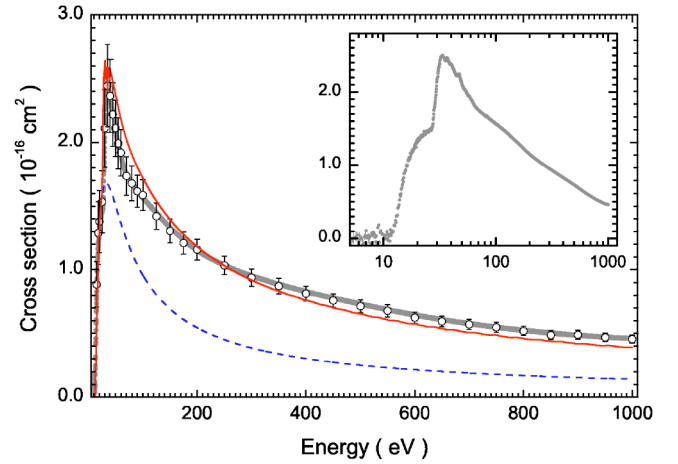
FIG. 2. Ionization cross sections for the $3p^63d4s$ configuration of Sc$^+$. The open circles denote measured absolute cross sections and the error bars comprise statistical as well as systematic uncertainties. Closely spaced gray points are the result of energy-scan measurements which were normalized to the absolute data points. The dashed line gives the configuration-average distorted-wave direct ionization cross section, and the solid curve shows the configuration-average distorted-wave direct ionization cross section plus the R-matrix excitation-autoionization cross-section results. The inset shows the experimental energy-scan data on a logarithmic energy scale.

istic atomic structure code of Cowan [16], where the mass-velocity and Darwin terms may be included in the radial Schrödinger equation. The configuration-average distorted-wave method has been used previously to calculate the direct ionization cross section for Sc^{2+} [17].

The close-coupling R-matrix method has been described in some detail previously [14,15]. It has been used to determine the excitation cross sections for Sc^{2+} [17], with reasonable agreement being found between theory and experiment. For the R-matrix calculations reported here, we use the parallel versions of the RMATRIX I suite of codes [18].

IV. RESULTS

Absolute cross sections for the single ionization of Sc$^+$ ions were measured between 15 and 1000 eV. In addition, a detailed energy scan between 6.5 and 1000 eV was performed. Results from both measurements are displayed in Fig. 2 together with the present theory calculation, i.e., the total EA cross section from the R-matrix calculation combined with the CADW direct ionization cross section. Note that we assume a 100% Auger yield for the autoionizing terms. All of the terms of the $3p^53d^24s$ configuration lie above the ionization threshold. Considering that this standard R-matrix calculation does not include continuum-coupling approximations [19], there is good agreement at all energies. We note that the R-matrix results are trending slightly below the experimental results at the highest energies. Based on the inset plot which shows the experimental scan data on a logarithmic energy scale, we also note that the shape of the cross-section feature between about 30 eV and 70 eV is reminis-
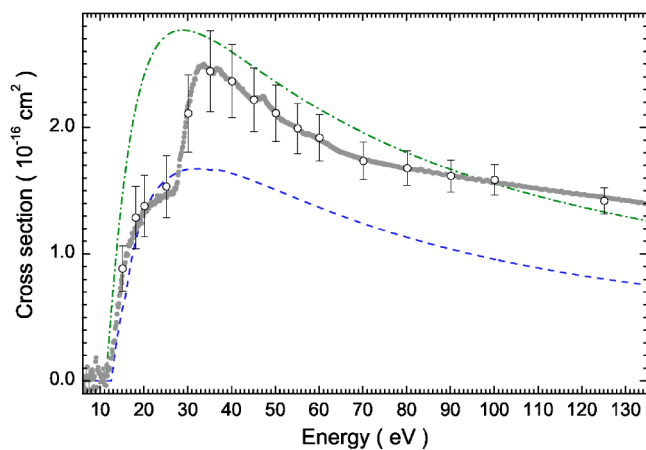
FIG. 3. Ionization cross sections for Sc⁺. The circles show the experimental results, the dashed line gives the configuration-average distorted-wave direct ionization cross section for the $3p^63d4s$, and the dot-dashed line gives the theoretical cross section for the excited $3p^63d^2$ configuration.

cent of the strong $4d \rightarrow 4f$ excitations in xenon and its neighboring elements (see, for example, Ref. [20]).

Among the possible direct ionization channels, only the $4s$ and $3d$ subshells contribute to single ionization. Figure 3 shows a comparison with experiment for the configuration-average distorted-wave direct ionization cross section for both the $4s$ and $3d$ subshells. It can be seen that theory matches well with experiment for the onset of the direct ionization cross section, and up to the onset of the excitation-autoionization cross section at 25 eV, indicating that the CADW approach is providing a reasonable estimate of the direct ionization cross section. It should also be noted that the CADW direct ionization cross section remains significantly below experiment even at 500 eV, indicating that the excitation cross section to autoionizing terms remains significant even at high energies. Figure 3 also shows the CADW direct-ionization cross section from the $3p^63d^2$ configuration, which is the first excited configuration to contain metastable terms. Although the $3p^63d^2$ results are in reasonable agreement with the peak height of the experimental cross section, it is clearly overestimating the direct ionization contribution, since the onset of the cross section at about 25 eV is characteristic of excitation autoionization, rather than direct ionization. Thus, any metastable presence in the experiment is likely to be small.

From CADW excitation cross-section calculations, it was seen that the largest contribution to the excitation-autoionization cross section is likely to be from the $3p^63d4s \rightarrow 3p^53d^24s$ transition. The CADW method significantly overestimates the excitation cross section for this transition. Therefore, we performed an R-matrix calculation for transitions between the terms of these two configurations. We used the parallel implementation of the R-matrix suite of codes [18] to evaluate the excitation cross section to autoionizing terms. Note that we included the $3p^63d4s$ ground configuration (two terms), $3p^63d^2$ and $3p^63d4p$ excited configurations (five terms and six terms, respectively), and the $3p^53d^24s$ autoionizing configuration (38 terms) in our close-

TABLE I. Selected calculated term energies of the $3p^63d4s$ and $3p^53d^24s$ configurations.

Configuration	Term	Energy with respect to the ground term (eV)
$3p^63d4s$	^3D	0.00
$3p^63d4s$	^1D	0.70
$3p^53d^24s$	^3F	35.88
$3p^53d^24s$	^3P	38.68
$3p^53d^24s$	^3D	39.62

coupling calculation. It was found that the largest excitation cross section arose from three dipole-allowed transitions to the $3p^53d^24s$ configuration, namely $3p^63d4s\,^3D \rightarrow 3p^53d^24s\,^3F$, ^3P, and ^3D. Table I gives the energies for these excited terms. Figure 4 shows our total R-matrix excitation cross-section results for excitation to the 38 terms of the $3p^53d^24s$ configuration, along with the individual contributions due to excitations to these three terms. It can be seen that these dipole transitions remain strong even at high energies, which is consistent with the contribution due to excitation autoionization inferred from the comparison between experiment and our direct ionization cross-section results. The CADW result is not shown, but has a sharp peak at about 40 eV of $\sim 4.7 \times 10^{-16}$ cm², and even at 100 eV it still lies significantly higher than the R-matrix cross section with a value of 1.5×10^{-16} cm².

Figure 5 shows the data of Fig. 2 with a reduced energy range, in order to examine the excitation-autoionization contribution in more detail. For a realistic comparison between theory and experiment, the R-matrix calculation has been convoluted with a 0.5 eV FWHM Gaussian to simulate the experimental energy spread. The threshold for direct single ionization of Sc⁺ by removal of the outer $4s$ electron is at 12.7998 eV [21]. Up to an energy of 27 eV, the cross section
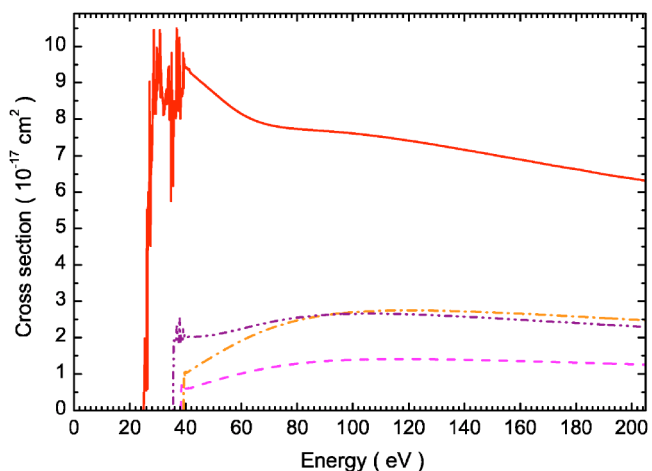
FIG. 4. Excitation cross sections for $3p^63d4s \rightarrow 3p^53d^24s$ transitions. The solid line shows the total R-matrix cross-section results to this excited configuration. The dashed line shows the R-matrix cross section for excitation to the $3p^53d^24s\,^3P$ term, the dot-dashed line excitation to the $3p^53d^24s\,^3D$ term, and the dot-dot-dashed line the excitation to the $3p^53d^24s\,^3F$ term.
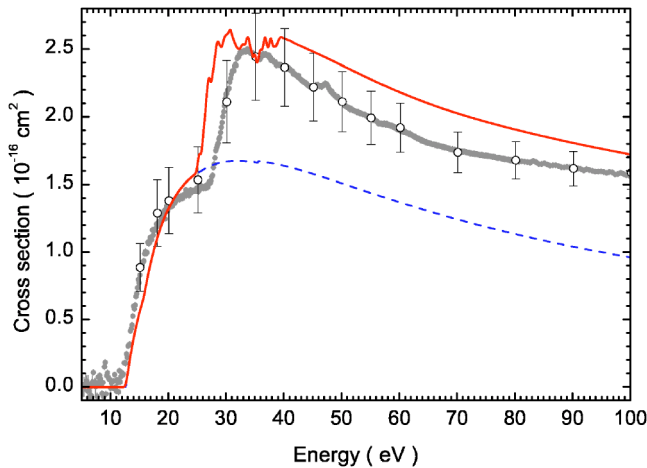
FIG. 5. Ionization cross sections for the $3p^63d4s$ configuration of Sc$^+$. The energy scan measurement (gray points) was normalized to the absolute data points (open circles). The dashed line gives the configuration-average distorted-wave direct ionization cross section, and the solid curve shows the configuration-average distorted-wave direct ionization cross section plus the R-matrix excitation-autoionization cross-section results. In this plot, the theoretical results have been convoluted with a 0.5 eV FWHM Gaussian to simulate the experimental energy distribution.

exhibits the typical structureless energy dependence of direct ionization, i.e., a steep rise at threshold up to a maximum and a slow decrease at higher energies. This energy dependence is represented by a CADW calculation (dashed line in Fig. 5). The calculated onset of the EA process is visible around 27 eV. Above 27 eV, the cross section rises abruptly from 1.5×10^{-16} cm^2 to 2.50×10^{-16} cm^2 at 33.7 eV. This rise is due to indirect processes involving the excitation of a $3p$ electron. At about 47 eV, the experimental data show clear evidence of an additional indirect ionization contribution which is attributed to (most probably resonant) excitation of the $3s$ subshell.

The value of ~40% for the contribution by indirect processes to the total ionization cross section is unusually high for a relatively light singly charged ion. Although the R-matrix calculation matches the height of the EA process within the total error bar, there is an obvious difference of $2-3$ eV in the threshold energy for this additional ionization channel. The experimental uncertainty of the relative energy is at most 1 eV in that range. The reason for the slight discrepancy is due to the difficulties in calculating level energies of doubly excited states in ions like the present one. Obtaining the strengths of the strong $3p \rightarrow 3d$ dipole transitions was the main purpose of the present analysis. They are much easier to get than their energy positions. Despite the minor differences between experiment and theory, for a complex species such as Sc$^+$, the level of agreement between theory and experiment is very good.

V. SUMMARY

We present a comparison between experimental measurements and theory for the electron-impact single ionization of Sc$^+$. Considering the complexity of the system, remarkably good agreement is found over a large energy range using configuration-averaged distorted-wave theory for the direct ionization and R-matrix theory for the excitation cross sections to autoionizing terms. The dominant contribution to excitation autoionization was found to be from three strong dipole allowed excitation transitions, namely $3p^63d4s\ ^3D \rightarrow 3p^53d^24s\ ^3F$, ^3P, and ^3D.

[1] J. Linkemann, A. Müller, J. Kenntner, D. Habs, D. Schwalm, A. Wolf, N. R. Badnell, and M. S. Pindzola, Phys. Rev. Lett. **74**, 4173 (1995).

[2] G. Hofmann, A. Müller, K. Tinschert, and E. Salzborn, Z. Phys. D: At., Mol. Clusters **60**, 113 (1990).

[3] A. Müller, K. Tinschert, G. Hofmann, E. Salzborn, and G. Dunn, Phys. Rev. Lett. **61**, 70 (1988).

[4] A. Müller, K. Huber, K. Tinschert, R. Becker, and E. Salzborn, J. Phys. B **18**, 2993 (1985).

[5] A. Müller, in *Physics of Ion-Impact Phenomena*, edited by D. Mathur, Springer Series in Chemical Physics, Vol. 54 (Springer, Berlin, 1991), pp. 13–90.

[6] S. Schippers *et al.*, Phys. Rev. Lett. **89**, 193002 (2002).

[7] P. Defrance, F. Brouillard, W. Claeys, and G. V. Wassenhove, J. Phys. B **14**, 103 (1981).

[8] A. Müller, K. Tinschert, C. Achenbach, R. Becker, and E. Salzborn, Nucl. Instrum. Methods Phys. Res. B **10**, 204

(1985).

[9] H. Teng, H. Knopp, S. Ricz, S. Schippers, K. A. Berrington, and A. Müller, Phys. Rev. A **61**, 060704 (2000).

[10] C. Becker, H. Knopp, J. Jacobi, H. Teng, S. Schippers, and A. Müller, J. Phys. B **37**, 1503 (2004).

[11] F. Brötz, R. Trassl, R. W. McCullough, W. Arnold, and E. Salzborn, Phys. Scr., T **92**, 278 (2001).

[12] K. Rinn, A. Müller, H. Eichenauer, and E. Salzborn, Rev. Sci. Instrum. **53**, 829 (1982).

[13] M. S. Pindzola, D. C. Griffin, and C. Bottcher, *Atomic Processes in Electron-Ion and Ion-Ion Collisions*, Vol. 145 of *NATO Advanced Study Institute, Series B: Physics*, edited by F. Brouillard (Plenum, New York, 1986).

[14] K. A. Berrington, W. B. Eissner, and P. H. Norrington, Comput. Phys. Commun. **92**, 290 (1995).

[15] V. M. Burke, P. G. Burke, and N. S. Scott, Comput. Phys. Commun. **69**, 76 (1992).

[16] R. D. Cowan, *The Theory of Atomic Structure and Spectra* (University of California Press, Berkeley, 1981).

[17] M. S. Pindzola, T. W. Gorczyca, N. R. Badnell, D. C. Griffin, M. Stenke, G. Hofmann, B. Weissbecker, K. Tinschert, E. Salzborn, A. Müller, and G. H. Dunn, Phys. Rev. A **49**, 933 (1994).

[18] D. M. Mitnik, D. C. Griffin, C. P. Ballance, and N. R. Badnell, J. Phys. B **36**, 717 (2003).

[19] C. P. Ballance and D. C. Griffin, J. Phys. B **37**, 2943 (2004).

[20] C. Achenbach, A. Müller, E. Salzborn, and R. Becker, Phys. Rev. Lett. **50**, 2070 (1983).

[21] S. Johansson and U. Litzen, Phys. Scr. **22**, 49 (1980).